



Detection and quantification of gas-phase oxidized mercury compounds by GC/MS

Colleen P. Jones¹, Seth N. Lyman¹, Daniel A. Jaffe², Tanner Allen¹, and Trevor L. O'Neil¹

¹Bingham Research Center, Utah State University, Vernal, UT 84078, USA

²University of Washington-Bothell, Bothell, WA 98011, USA

Correspondence to: Seth N. Lyman (seth.lyman@usu.edu)

Received: 28 January 2016 – Published in Atmos. Meas. Tech. Discuss.: 29 February 2016

Revised: 26 April 2016 – Accepted: 27 April 2016 – Published: 18 May 2016

Abstract. Most mercury pollution is emitted to the atmosphere, and the location and bioavailability of deposited mercury largely depends on poorly understood atmospheric chemical reactions that convert elemental mercury into oxidized mercury compounds. Current measurement methods do not speciate oxidized mercury, leading to uncertainty about which mercury compounds exist in the atmosphere and how oxidized mercury is formed. We have developed a gas chromatography/mass spectrometry (GC-MS)-based system for identification and quantification of atmospheric oxidized mercury compounds. The system consists of an ambient air collection device, a thermal desorption module, a cryofocusing system, a gas chromatograph, and an ultra-sensitive mass spectrometer. It was able to separate and identify mercury halides with detection limits low enough for ambient air collection (90 pg), but an improved ambient air collection device is needed. The GC/MS system was unable to quantify HgO or Hg(NO₃)₂, and data collected cast doubt upon the existence of HgO in the gas phase.

1 Introduction

Mercury (Hg) emitted in the gas phase can remain in the Earth's atmosphere for many months and be transported around the globe (Lindberg et al., 2007). Atmospheric Hg pollution is a global problem, and regulation of Hg emissions exist at the state, national, and international levels (Selin, 2009). Hg pollution arises from a variety of natural and anthropogenic point and nonpoint sources (Gustin et al., 2008; Seigneur et al., 2004). Hg can exist in the atmosphere as elemental Hg (Hg⁰), or as various oxidized Hg compounds

(Hg^{II}) (Lyman et al., 2010a). Most mercury is emitted to the atmosphere as Hg⁰ (Pacyna et al., 2006), but it can be oxidized to Hg^{II} in the atmosphere, and Hg^{II} can be reduced to Hg⁰ (Hedgecock and Pirrone, 2004). Hg^{II} can be found in both the particulate-bound (Hg_p^{II}) and gaseous forms (Hg_g^{II}) (Sprovieri et al., 2010) and is water-soluble and semi-volatile (Gustin et al., 2008; Lindberg et al., 2007). As a result, aerosols and clouds readily absorb Hg_g^{II}, and it is also readily dry deposited (Holmes, 2012; Lyman et al., 2007). Lyman and Jaffe (2012) and others (Gratz et al., 2015; Slemr et al., 2009; Talbot et al., 2007) report that the upper troposphere and lower stratosphere are depleted in Hg⁰ and enriched in Hg^{II}, and oxidation of Hg⁰ to Hg^{II} has also been shown to occur in the marine boundary layer (Wang et al., 2014) and the Arctic during springtime (Steffen et al., 2008). The location and timing of Hg deposition to ecosystems depends on atmospheric chemistry and the form of Hg in the air (Gustin et al., 2013b; Holmes et al., 2010; Lin et al., 2006; Lyman and Gustin, 2008; Lyman et al., 2010a).

In 1974, Johnson and Braman (1974) suggested that oxidized Hg might consist of HgO and/or Hg halides, and most current studies still echo this hypothesis (Ariya et al., 2009; Holmes et al., 2010; Hynes et al., 2009; Lin et al., 2006). HgO could be produced by the reaction of Hg⁰ with ozone (Pal and Ariya, 2004b), OH (Pal and Ariya, 2004a), or NO₃ (Sommar et al., 1997). Evidence exists for the involvement of NO₃ in formation of Hg^{II} (Peleg et al., 2015). Some have argued that HgO is likely to exist only as Hg_p^{II} (Calvert and Lindberg, 2005; Shepler and Peterson, 2003) and that oxidation of Hg⁰ by ozone may produce an HgO₃ intermediate which could decompose to HgO on particles (Calvert and Lindberg, 2005) or react with water to form Hg(OH)₂ (Tos-

sell, 2006). Seigneur et al. (1994) suggested that $\text{Hg}(\text{OH})_2$ could be produced from the reaction of Hg^0 with H_2O_2 .

Reactive halogen species, especially bromine species, have received attention as potential Hg^0 oxidants since the discovery of Hg depletion events associated with “bromine explosions” during Arctic spring (Schroeder et al., 1998; Steffen et al., 2008), and HgBr_2 and/or HgBrOH have been hypothesized as products (Holmes et al., 2006). Halogen radicals have also been implicated as potential Hg oxidants in the marine boundary layer (Laurier et al., 2003), the Dead Sea (Obrist et al., 2011), and the free troposphere and stratosphere (Holmes et al., 2006).

Hg^{II} emitted from combustion facilities is generally thought to be HgCl_2 (Galbreath and Zygarlicke, 2000; Wilcox and Blowers, 2004). Some oxidized Hg in the atmosphere may be methylmercury, but less than 3 % of oxidized Hg in rainwater is methylated (Lindberg et al., 2007), and it is likely that most atmospheric Hg^{II} is inorganic.

Hg^0 , Hg_p^{II} , and Hg_g^{II} (operationally defined) are measured routinely at dozens of locations around the world. Current measurement methods for Hg_g^{II} have been shown to be biased low, however (Gustin et al., 2013a; McClure et al., 2014), and ozone and water vapor have been implicated as interferences (Huang and Gustin, 2015; Lyman et al., 2010b). These measurements have only been calibrated rarely, and development and regular deployment of a field-deployable calibrator has been called for (Gustin et al., 2013b; Jaffe et al., 2014). Current Hg^{II} instrumentation is also not species-specific, so it does not provide information about the individual compounds that make up measured Hg^{II} (Jaffe et al., 2014). Different species will have different deposition rates, solubility, and bioavailability (Eagles-Smith and Ackerman, 2014; Peterson et al., 2015), so determining the chemical nature of Hg^{II} is a critical research priority (Gustin et al., 2013b; Jaffe et al., 2014; Malcolm and Keeler, 2007). Huang et al. (2013b) have developed a thermal desorption system to provide chemical information about Hg_g^{II} , but other, complimentary methods are also needed.

Unlike the atomic fluorescence method commonly used for measurement of atmospheric Hg, mass spectrometric methods can be used to identify the chemical composition of Hg compounds (Deeds et al., 2015). Further, gas chromatography/mass spectrometry (GC/MS) can allow for separation of individual Hg compounds and separation of Hg compounds from non-mercury components of ambient air samples (Babko et al., 2001; Olson et al., 2002). Inductively coupled plasma mass spectrometry (ICP-MS) is routinely used for measurement of Hg and Hg isotope ratios, but the method is only useful for elemental analysis (dos Santos et al., 2009). GC analysis is routinely used for analysis of organic Hg in various media, and for analysis of Hg^{II} in water after alkylation of the inorganic Hg compounds (Cavalheiro et al., 2014). However, alkylation destroys the native structure of Hg compounds and thus does not provide information about their original identity.

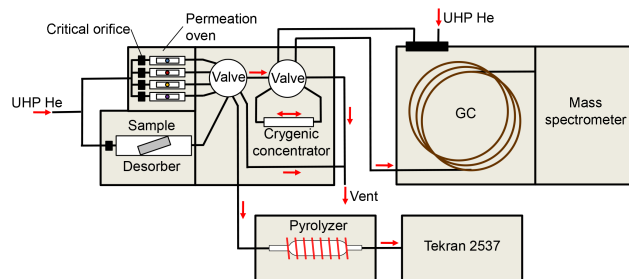


Figure 1. Diagram of GC/MS system used to identify Hg compounds, and a pyrolyzer and Tekran 2537 system to quantify the amount of Hg compounds generated by the permeation oven.

Babko et al. (2001) showed that GC/MS could be used to separate and identify Hg halides. They injected a solution of HgCl_2 in acetone into a GC/MS and found good recovery and consistent peaks. The detection limits, however, were much higher than would be practical for ambient air analysis. Olson et al. (2002) used GC/MS to identify Hg^{II} generated by an MnO_2 sorbent in simulated flue gas. They used an impinger to trap the Hg in acetonitrile, then evaporatively concentrated the solution before injecting into a GC/MS. They injected HgCl_2 in acetonitrile and observed mass spectra that were clearly indicative of HgCl_2 . They also injected $\text{Hg}(\text{NO}_3)_2$ and $\text{Hg}(\text{NO}_3)_2 \times \text{H}_2\text{O}$ and saw a similar peak and mass spectra to what they observed in the gas that passed through the MnO_2 sorbent.

We have developed a GC/MS-based system to quantify and chemically identify Hg compounds. We describe this analytical system in detail, provide first results, and discuss remaining challenges.

2 Materials and methods

The GC/MS-based Hg^{II} detection system consisted of a sample collector to concentrate Hg compounds from the ambient atmosphere, a sample desorber to introduce collected compounds into the gas phase, a cryogenic preconcentrator (cryotrap) to focus and inject Hg compounds, a gas chromatograph to separate Hg compounds from each other and from possible interferences, and an ultra-sensitive mass spectrometer to definitively determine the chemical speciation of Hg compounds (Fig. 1). It also incorporated a permeation system, pyrolyzer, and Hg^0 detector to introduce a consistent, quantifiable amount of various Hg compounds to the system in the gas phase. All wetted parts of the system were kept at at least 160 °C (except the sample desorber, which was sometimes cooler), and all wetted parts except the GC columns and VICI GC valve rotors were composed of deactivated fused silica-coated stainless steel. The VICI GC valve rotors were composed of Valcon E (a polyaryletherketone/PTFE composite).

2.1 Sample collector

Four collection materials were tested for suitability to concentrate volatile Hg compounds in air samples. Collection materials tested were nylon membranes, polydimethylsiloxane (PDMS) sorption tubes, quartz wool-filled tubes, and deactivate fused silica-coated stainless steel. Nylon membranes were Cole-Parmer nylon polyamide membranes (47 mm round, 0.2 μm thick, P/N: EW-36229-04). The PDMS sorption tubes were those for a Gerstel Thermal Desorption Unit (TDU), and were filled with conditioned PDMS foam (P/N: 013758-105-00). Quartz wool-filled tubes were made from 22 cm long \times 1.3 cm diameter perfluoroalkoxy (PFA) tubing that was washed with soap and water, soaked for 24 h in a 10 % nitric acid bath, rinsed with 18.2 M Ω cm⁻¹ water, then dried in a particle-free environment. The tubing was then filled with quartz wool that had been baked at 800 °C for 2 h to ensure no contamination. Deactivated fused silica-coated stainless steel was a 1 cm length of 0.3 cm tubing.

Selection of the best collection surface was based on presence of identifiable Hg peaks on the GC/MS with the least amount of signal interference. Hg was introduced to the sample collectors either from the permeation oven or by passing outdoor ambient air through the collectors. Ambient air samples were collected from Peavine Peak (latitude 39.590, longitude -119.929) near Reno, Nevada; at the University of Nevada, Reno campus in Reno, Nevada (latitude 39.537, longitude -119.805); and Grizzly Ridge (latitude 40.738, longitude -109.484) near Vernal, Utah, using quartz wool-filled tubes and nylon membranes. Quartz wool-filled tube ambient air samples were collected by pulling air through the tubes at 30 L min⁻¹ for 3 h. Some of the tubes were at ambient temperature during collection, while others were kept at 0 °C. Nylon membranes were collected by pulling air through the membranes at 1 L min⁻¹ for 2 weeks. More information about nylon membrane methods is available from Huang et al. (2013a). All ambient air samples were collected during summer months.

2.2 Sample desorber

A thermal desorption module was used to reintroduce collected compounds into the gas phase. We constructed this module by connecting a lab oven to an adjustable digital temperature controller. Membrane samples were placed within a sample desorption chamber inside the oven, while sample collection tubes were connected directly to the desorption flow path. The desorption chamber was stainless steel coated with deactivated fused silica. A constant flow of ultra-high purity (UHP) Helium (He) acted as a carrier gas to pass volatilized compounds to the cryotrap. The flow of UHP He was controlled at a rate of 30 mL min⁻¹. Desorption temperatures in the range of 80–160 °C were used.

2.3 Cryogenic preconcentrator

The cryogenic preconcentrator (cryotrap) was used to focus desorbed compounds prior to introduction into the GC. A Scientific Instrument Services Model 961 GC Cryo-Trap was used with liquid nitrogen as the cryogen. The cryotrap works by enclosing a portion of the GC column in a small metal cylinder. A flow of liquid nitrogen is passed through the small cylinder at a rate determined by a digital temperature controller. Volatile compounds are retained on the cooled column. After collection, the metal cylinder rapidly heats up via a nichrome wire heating coil, volatilizing concentrated compounds and allowing them to pass into the GC/MS. During this step, the trap temperature is able to increase by 14 °C per second. Cryotrap cooling temperatures tested ranged from -50 to 30 °C, and heating temperatures tested ranged from 170 to 240 °C. The cryotrap was housed in a lab oven. Lab oven temperatures tested ranged from 160 to 220 °C. A VICI six-port GC valve (Model 4C6WT) was housed within the lab oven and controlled flow of sample to the cryotrap, and from the cryotrap to the GC. A heated line with a deactivated fused silica guard column (0.25 mm internal diameter) was used to connect the cryotrap to the GC.

2.4 Gas chromatograph with an ultra-sensitive mass spectrometer

A Shimadzu GC-2010 Plus gas chromatograph was used to separate Hg compounds from each other and from possible interferents. Different GC column types and lengths were used to test optimum conditions for Hg compound separation. A 30 m low-polarity Restek Rxi-5Sil MS column (5 % diphenyl/95 % dimethyl polysiloxane), a 60 m ultra-low-polarity Supelco SPB-Octyl fused silica capillary column (50 % *n*-Octyl/50 % methyl siloxane), and a 30 m non-polar Restek Rxi-1ms column (100 % dimethyl polysiloxane) were tested. GC oven temperatures tested ranged from 140 to 220 °C. After passing through the GC column, the compounds of interest moved to a Shimadzu QP2010 Ultra mass spectrometer for detection of unique chemical signatures of Hg compounds in samples. The MS was operated in high-sensitivity electron impact ionization mode, and included a direct probe inlet. Small quantities of solid-phase Hg compounds were added directly to the MS via to the direct probe inlet to determine representative mass spectra for the compounds.

2.5 Permeation system, pyrolyzer, and Hg detector

Permeation tubes were made to generate four Hg^{II} compounds (HgBr₂, HgCl₂, Hg(NO₃)₂, and HgO; Sigma-Aldrich, purity 99.9 % or greater). These compounds were packed in permeation tubes constructed of thin-wall 0.3 cm diameter FEP tubing with solid polytetrafluoroethylene (PTFE) plugs in both ends. The permeable length

of each tube was approximately 1 mm. Larger permeation tubes (1.3 cm diameter \times 15 cm permeable length) were also tested for $\text{Hg}(\text{NO}_3)_2$ and HgO . Permeation tubes were enclosed within 0.5 cm inner diameter deactivated fused silica-coated stainless steel tubing. UHP He flowed at 30 mL min^{-1} through the stainless steel tubing and over the permeation tubes. The tubes were housed in an oven consisting of an insulated metal box heated to $100 \pm 0.1^\circ\text{C}$. A VICI multiport GC valve (Model CSF6) selected among four available permeation tubes or passed permeation flow to vent. The multiport valve was housed within the same lab oven as the cryotrap.

A pyrolyzer was used to verify permeation rates of Hg compounds. The pyrolyzer consisted of a 2.5 cm diameter \times 18 cm length quartz tube packed with quartz wool. The quartz tube was wrapped with nichrome wire that was used with a variable voltage controller to control the temperature of the tube. The pyrolyzer was kept at 800°C to convert Hg compounds to Hg^0 as they passed from the permeation oven through the quartz tube. Hg^0 concentrations were measured downstream of the pyrolyzer using a Tekran 2537 mercury vapor analyzer.

2.6 Hg compound transmission tests

We permeated HgBr_2 into a 1 cm diameter PFA manifold to test the ability of different materials to transmit Hg compounds (Fig. S1 in the Supplement). The manifold was heated to 100°C . Air scrubbed of Hg via an activated carbon cartridge was drawn through the manifold at 10 L min^{-1} . A tee pulled a 1 L min^{-1} subset of air from this manifold into a Tekran 2537/1130 speciation system with a KCl-coated denuder, which measured Hg^0 and Hg^{II} . The tee to the denuder was 100 cm downstream of the point where HgBr_2 was added to the manifold air. One of several 15 cm long \times 0.3 cm diameter tubes was placed between the manifold and the Tekran speciation system to test the ability of these tubes to transmit HgBr_2 . These 15 cm tubes were constructed of different materials, including stainless steel, PFA (as a control, since the entire manifold was PFA), PEEK, and deactivated fused silica-coated stainless steel. Fittings used to secure the 15 cm tubes were of the same materials as the tubes. The 15 cm stainless steel, PFA, PEEK, and deactivated fused silica-coated stainless steel tubes were each tested for 24 h. The Tekran system collected one measurement every 1.5 h, so approximately 16 samples were obtained for each experimental condition.

3 Results and discussion

We initially identified HgBr_2 and HgCl_2 via the method utilized by Babko et al. (2001), which was to dissolve the compounds in acetone and inject the solution into a splitless inlet at 200°C . We used a non-polar 100% PDMS column at 160°C for separation. We were able to separate HgCl_2 from HgBr_2 with this system (Fig. 2). The relative abun-

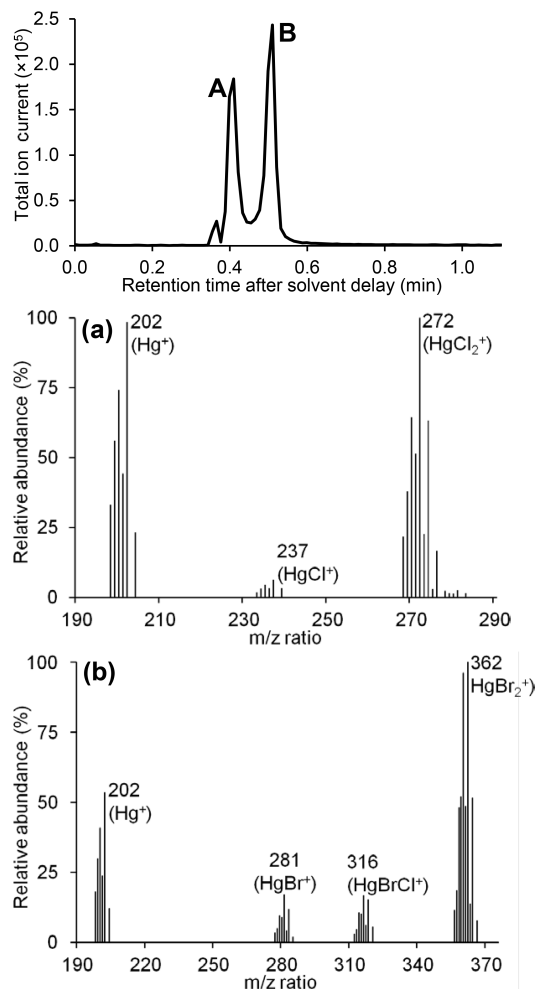


Figure 2. Chromatogram of a mixed standard of HgCl_2 and HgBr_2 in acetone ($0.5 \mu\text{g } \mu\text{L}^{-1}$ for each compound) (top), mass spectra for HgCl_2 (b, middle) and HgBr_2 (b, bottom). Solvent delay was 2 min.

dance of Hg isotopes in Fig. 2 is similar to isotopic abundances reported by IUPAC (de Laeter et al., 2004), confirming the identification. The detection limit of HgCl_2 analyzed by this method, calculated as 3 times the standard deviation of seven injections near the detection limit, was 9 ng, much too high for ambient air detection of mercury compounds. Replicate injections showed a high degree of variability (relative standard deviation of 30 to 45%). The manual syringe used for injections became permanently contaminated with HgBr_2 and HgCl_2 after use, so we expect that much of the observed variability was due to retention and interactions on the syringe walls, as well as the walls of the injection port.

To eliminate the variability created by liquid injections of these very reactive compounds, we developed the system described in Methods. We tested a number of different configurations and materials to determine the method most likely to allow for identification of Hg^{II} in ambient air.

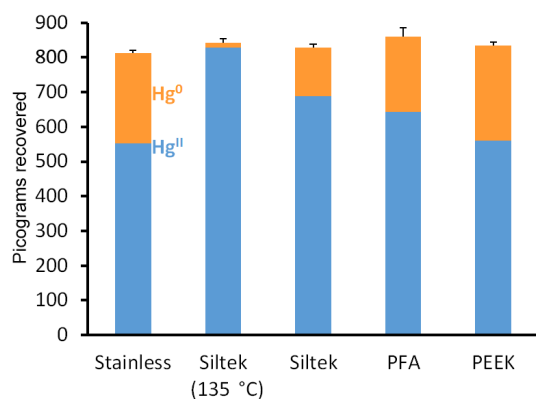


Figure 3. Picograms of Hg^{II} and Hg⁰ recovered when HgBr₂ was permeated into mercury-free air and passed through a 15 cm section of 0.3 cm diameter tubing constructed of the materials indicated. Tubing was kept at 110–115 °C, except when indicated otherwise. “Siltek” indicates stainless steel tubing coated with Siltek-brand deactivated fused silica. Whiskers represent 95 % confidence intervals.

3.1 System materials and temperatures

As a first step in the development of the system, we tested the ability of stainless steel, deactivated fused silica-coated stainless steel (Siltek brand), PFA, and PEEK tubing to transmit gas-phase HgBr₂. The lowest Hg^{II} recovery (and highest Hg⁰) was observed with stainless steel tubing, followed by PEEK (Fig. 3). Deactivated fused silica-coated stainless steel performed better than PFA, with more Hg^{II} and less Hg⁰ observed. The amount of total Hg recovered was the same whether deactivated fused silica-coated stainless steel was heated to 135 or 110–115 °C ($p = 0.39$; the manifold used for these tests was not capable of achieving more than 135 °C), but the percentage of recovered Hg that was Hg^{II} increased from 83 to 98 %. It is not clear why the 15 cm deactivated fused silica-coated stainless steel tube at 135 °C resulted in such an improved Hg^{II} : Hg⁰ ratio relative to the 15 cm PFA tubing, since a relatively short length of coated stainless tubing was used in a manifold that was otherwise constructed entirely of PFA, and some decomposition of Hg^{II} to Hg⁰ would be expected in the remainder of the manifold even if the 15 cm tube did not lead to any decomposition. More study of Hg compound decomposition in the presence of different materials is warranted.

It appears from Fig. 3 that cooler temperatures and less suitable tubing materials led to the conversion of HgBr₂ to Hg⁰, perhaps due to reactions facilitated by or on the materials themselves. Others have reported that higher temperatures allow for increased transmission of Hg halides without significant decomposition to Hg⁰ (Lyman et al., 2010b). Wilcox and Blowers (2004) determined a theoretical temperature-dependent rate constant for the decomposition of HgCl₂ ($\text{HgCl}_2 + \text{M} \leftrightarrow \text{HgCl} + \text{Cl} + \text{M}$), and compared those results to rate constants developed from exper-

Table 1. GC/MS results from permeation of HgBr₂ with varying GC oven, valve oven, and line temperatures. Each iteration was performed at least in duplicate to verify the consistency of results. Peak area and height are for m/z 362.

GC oven temp. (°C)	Retention time	Peak area	Peak height
140	5.91	11 794	802
160	4.52	14 676	1077
180	3.87	17 037	1158
200	2.66	22 892	1235
Valve oven and line temp. (°C)			
180	4.32	36 058	1989
200	4.19	40 646	1998

imental data (Widmer et al., 2000). Their theoretical rate equation predicts that HgCl₂ will be stable up to about 850 °C, while the rate equation determined from experimental data predicts HgCl₂ stability up to 450 °C (stable = less than half of initial HgCl₂ decomposed within 60 s). At 240 °C (the maximum temperature reached by any part of our GC/MS system), both rate equations predict $\ll 1$ % decomposition within 60 s. In addition, L’Vov (1999) showed minimal decomposition of HgO up to 450 °C.

We constructed the plumbing of our GC/MS system using deactivated fused silica-coated stainless steel where possible. After the system was constructed, we tested different system temperature settings, including temperatures of the oven that housed the VICI valves and the cryotrap, the temperature of the transfer line from the cryotrap to the GC, and the GC oven temperature. Table 1 shows that higher peak area and peak height were observed for higher GC oven, valve oven, and transfer line temperatures, up to 200 °C. These temperatures were optimized for HgBr₂, and additional work is needed to determine optimal system temperatures for other Hg compounds.

3.2 Cryogenic preconcentrator

Results of cryotrap cooling temperature tests are given in Table 2. While cryotrap cooling temperatures of 0 and −25 °C resulted in similar peak areas, peak heights were greater with 0 °C, probably because the higher temperature allowed for more rapid desorption when the cryotrap was heated. Peak area and shape deteriorated at cryotrap cooling temperatures above 0 °C. When analyzing ambient air samples, cryotrapping temperatures slightly above 0 °C may be ideal, since they would allow for efficient trapping of Hg compounds, but allow water to pass through. While HgBr₂ peaks were smaller when the cryotrap was cooled to −50 °C, this lower temperature allowed the cryotrap to efficiently collect Hg⁰ as well (data not shown).

Table 2. GC/MS results from permeation of HgBr₂ with varying cryotrap cooling and desorption temperatures. Each iteration was performed at least in duplicate to verify the consistency of results. Peak area and height are for *m/z* 362.

Cryotrap cooling temp. (°C)	Retention time	Peak area	Peak height
-50	4.21	104 386	4789
-25	4.22	137 471	7206
0	4.14	134 462	8623
5	4.14	117 864	8272
10	4.12	113 516	7589
30	4.13	39 526	1583
Cryotrap desorb temp. (°C)			
170	3.35	83 198	8582
200	4.14	101 757	8557
220	3.36	173 059	17 501
240	3.377	175 723	17 567

Hotter cryotrap desorption temperatures resulted in better peak areas for HgBr₂ (Table 2), with a desorption temperature of 240 °C resulting in the best peak area and peak shape. Hotter desorption temperatures likely resulted in more rapid volatilization of HgBr₂ from the cryotrap, leading to improved peak shape.

3.3 Chromatographic columns

Of the three columns we tested for transmission of HgBr₂, we only observed HgBr₂ peaks with the Rxi-5Sil MS column or the SPB-Octyl column. We observed consistent HgBr₂ peaks with the Rxi-1ms column. Babko et al. (2001) observed HgCl₂ peaks with a low-polarity column similar to the Rxi-5Sil MS column we used (DB-5; 5 % diphenyl/95 % dimethyl polysiloxane). Olson et al. (2002) only observed Hg compound peaks when using a 30 m non-polar phase column (DB1; 100 % dimethyl polysiloxane) similar to the Rxi-1ms column we used. Olson et al. (2002) were not able to observe Hg peaks with more polar columns that had polyethylene glycol, cyanopropyl phenyl, or trifluoropropyl phases.

3.4 Hg compound detection

The permeation rate for HgBr₂, determined by the pyrolyzer and Tekran analyzer system, was 37 pg s⁻¹. After incorporating the optimizations reported above, and after further optimizing the parameters of the mass spectrometer, permeation of 22.2 ng of HgBr₂ resulted in a peak area of 1 788 451 and a peak height of 143 238 when the MS was operated in selected ion mode for *m/z* 362 (Fig. 4). The HgBr₂ detection limit for the optimized system in selected ion mode, calculated as 3 times the standard deviation of replicate low-concentration

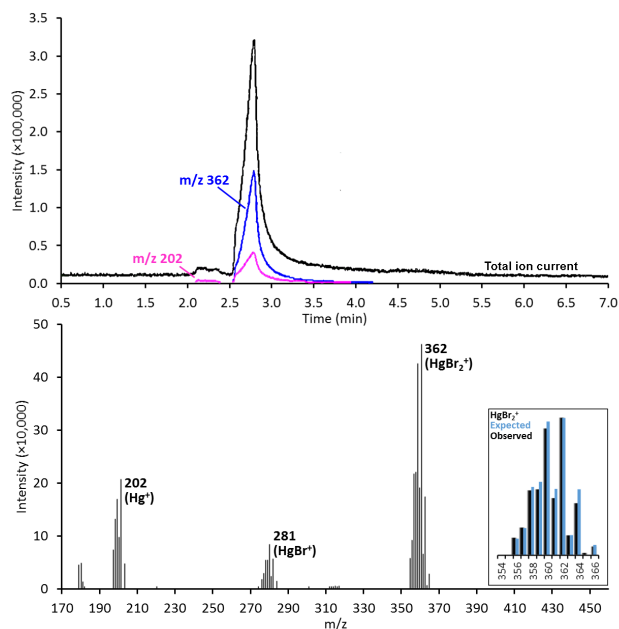


Figure 4. Chromatogram (above) and mass spectrum at 2.92 min (below) of HgBr₂ emitted from a permeation tube. The Y axis shows the mass spectrometer's ion current intensity. The box on the bottom right compares the expected HgBr₂⁺ mass spectrum (from de Laeter et al., 2004) to the observed spectrum.

samples, was 90 pg. The detection limit in scan mode was 300 pg.

A small, poorly formed Hg⁰ peak was often observed prior to Hg halide peaks in chromatograms (see *m/z* 202 trace in top of Fig. 4). This Hg⁰ peak was probably the result of breakdown of Hg halides to Hg⁰ within the chromatographic column, and its poor shape can be explained by continued breakdown as Hg halides moved through the column. The small size of the peak relative to the Hg halide peak is an indicator that Hg halide decomposition in the column was limited. Hg⁰ chromatographic peaks during Hg halide injections were not likely the result of Hg⁰ emitted from permeation tubes, since any Hg⁰ emitted or formed prior to the cryotrap would have passed through the cryotrap at its typical collection temperature of 0 °C.

While Hg⁰ was detected from Hg(NO₃)₂ and HgO-containing permeation tubes (when the cryotrap cooling temperature was lowered to -50 °C), we were unable to observe unequivocal Hg(NO₃)₂ or HgO mass spectra when analyzing the output of these permeation tubes with the GC/MS. A consistent peak with a prominent 218 *m/z* signal was observed at a retention time of about 10 min when Hg(NO₃)₂ or HgO was permeated (Fig. 5). While *m/z* 218 is the most abundant expected mass for HgO⁺, the observed isotope pattern did not indicate Hg. Instead, the mass spectrum for this peak was similar to mass spectra for siloxanes, indicating column or tubing degradation as the source. The absence of Hg in this

peak was confirmed by the lack of an Hg^+ signal at m/z 202 (Fig. 5).

Lyman et al. (2009) constructed HgO permeation tubes and found that, along with Hg^0 , an Hg compound was emitted from these tubes that could be collected and analyzed using KCl-coated denuders or cation-exchange membranes. Huang et al. (2013a) showed that, when collected on nylon membranes, the Hg compound emitted from HgO permeation tubes exhibited a thermal desorption profile that was different from those exhibited by HgCl_2 , HgBr_2 , and Hg^0 . They showed that $\text{Hg}(\text{NO}_3)_2$ permeation tubes also emit a reactive Hg compound. It is not known, however, whether the Hg compound emitted from HgO permeation tubes is HgO . Huang et al. (2013a) proposed that the emitted compound could be Hg_2O . Regardless of the chemical identity of the compound, it is possible that we were not able to detect it because it degraded within the system tubing, valves, or the chromatographic column. The GC/MS did not report any Hg signal, including Hg^0 , when analyzing the output from HgO and $\text{Hg}(\text{NO}_3)_2$ permeation tubes with a cryotrap temperature of 0°C . This indicates either (1) the Hg compound emitted from these permeation tubes degraded prior to or within the cryotrap, allowing Hg^0 to pass through the cryotrap and out of the system; (2) the emitted Hg compound is too volatile to collect on a cryotrap at 0°C , or (3) the emitted Hg compound becomes permanently bound to some part of the analytical system and does not degrade. System temperatures and materials were optimized for HgBr_2 , and different materials and/or a different temperature regime may improve detection for compounds emitted from HgO and $\text{Hg}(\text{NO}_3)_2$ permeation tubes.

We introduced small quantities of HgO and $\text{Hg}(\text{NO}_3)_2$ (separately) into the direct injection probe on the MS to determine a mass spectrum for these compounds. Figure 6 shows these mass spectra. Only Hg^+ was observed from the direct injection of HgO , and no significant signal was observed around m/z 218 (HgO^+) or m/z 420 (Hg_2O^+). This could be because (1) HgO is not volatile enough to produce enough vapor in the ionization chamber of the MS to result in a detectable signal, so only off-gassed Hg^0 was observed (as Hg^+) or (2) the ionization energy of the MS was so strong that all HgO was broken down to Hg^+ within the ionization chamber. HgO^+ was observed, however, when $\text{Hg}(\text{NO}_3)_2$ was inserted into the direct probe, probably as a breakdown product. This provides evidence that the MS could detect HgO as HgO^+ if it did indeed exist in the gas phase. The fact that it was not detected when solid HgO was inserted into the direct probe may indicate that HgO does not have an appreciable gas phase. If this is the case, it is not clear what is emitted from HgO permeation tubes that can be collected on nylon membranes and KCl-coated denuders (Huang et al., 2013a).

The mass spectrum for $\text{Hg}(\text{NO}_3)_2$ showed $\text{Hg}(\text{NO}_3)_2^+$ (m/z 326) and several breakdown products, including HgNO_3^+ (m/z 264), and HgO^+ (m/z 218). A cluster of peaks

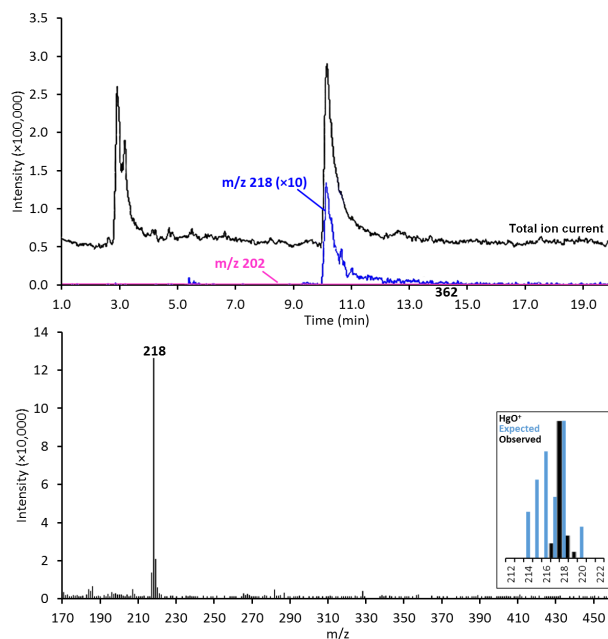


Figure 5. Chromatogram (above) and mass spectrum at 10.10 min (below) generated from analysis of 34 ng Hg emitted from an HgO permeation tube. The box on the bottom right compares the expected HgO^+ mass spectrum (from de Laeter et al., 2004) to the observed spectrum. While the prominent mass peak was m/z 218, the observed isotope pattern does not indicate HgO^+ .

around m/z 343 was also observed and could be interpreted as the monohydrate of $\text{Hg}(\text{NO}_3)_2$. Olson et al. (2002) dissolved $\text{Hg}(\text{NO}_3)_2$ in acetonitrile and interpreted resultant mass spectra to be caused by reaction of $\text{Hg}(\text{NO}_3)_2$ with column material, producing CH_3HgCl . Our direct probe results suggest the existence of gas-phase $\text{Hg}(\text{NO}_3)_2$ and do not match the spectra presented by Olson et al. (2002).

3.5 Laboratory tests of sample collection materials

We permeated Hg compounds onto nylon membranes and into PDMS foam-filled tubes, quartz wool-filled tubes, and deactivated fused silica-coated tubes and used the sample desorption oven to transmit collected Hg compounds onto the cryotrap and then into the GC/MS. When we heated nylon membranes to 100°C or greater in the desorption oven, the prominent observed peak was consistent with dodecanoic acid, a potential degradation product of the nylon material (Carragher, 2014). Dodecanoic acid exhibits prominent peaks at and near m/z 200, and the dodecanoic acid peak intensity was so high as to obscure any Hg peaks when loaded in the laboratory or when sampling ambient air. Huang et al. (2013a) used nylon membranes to collect Hg compounds and desorbed those compounds into a pyrolyzer and atomic fluorescence analyzer. The atomic fluorescence instrument only detects Hg^0 , however, so interference from nylon breakdown products was not an issue.

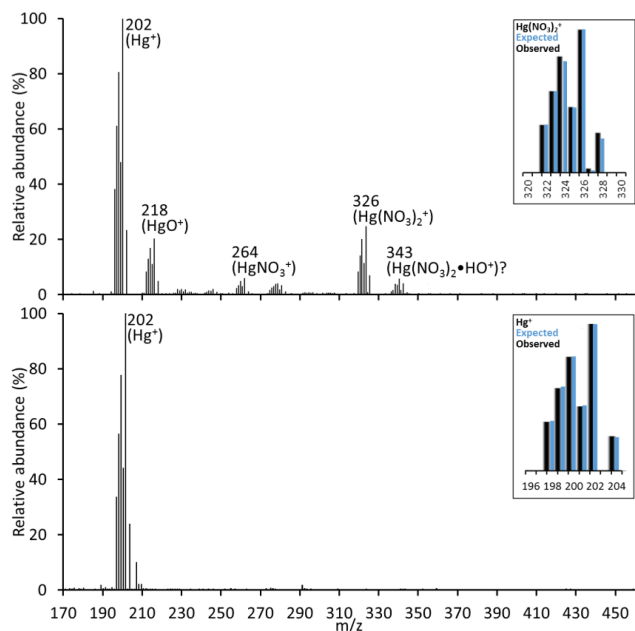


Figure 6. Mass spectrum for $\text{Hg}(\text{NO}_3)_2$ (above) and HgO (below) derived from direct probe injection into the MS. The boxes at top left in each pane compare the expected indicated mass spectrum (from de Laeter et al., 2004) to the observed spectrum.

Like nylon membranes, PDMS foam-filled tubes also had too much interference to allow for detection of Hg compounds, even when loaded with as much as 60 ng HgBr_2 .

Quartz wool-filled PFA tubes exhibited less interference and clearly identifiable Hg halide signals (Fig. 7). However, chromatograms from quartz wool-filled tubes had poorly shaped peaks and substantial non-Hg signal. The cause of the poorly shaped peaks is not known. Quartz particles could have accumulated in the cryotrap, causing a slow desorption of Hg compounds during cryotrap heating. If this occurred, the quartz particles were apparently cleaned out after each analysis, since we performed injections of Hg halides directly from the permeation oven onto the cryotrap subsequent to quartz wool analyses and observed normal chromatographic peaks.

While HgCl_2 was loaded onto a quartz wool-filled tube for the analysis shown in Fig. 7, the figure shows some HgBr_2 signal in the mass spectrum. The quartz wool-filled tube had previously been loaded with HgBr_2 , and some residual HgBr_2 apparently remained in the tube. Additionally, a cluster of masses centered at m/z 316, corresponding with HgBrCl , can be clearly observed in the mass spectrum. The same cluster of masses can be seen in part B of Fig. 2 and in Fig. 4. HgBrCl could exist because of (1) a reaction between HgCl_2 and HgBr_2 in the acetone solution in Fig. 2 or on the quartz wool in Fig. 7, or (2) it could be a contaminant in the commercial Hg halide compounds used in this study.

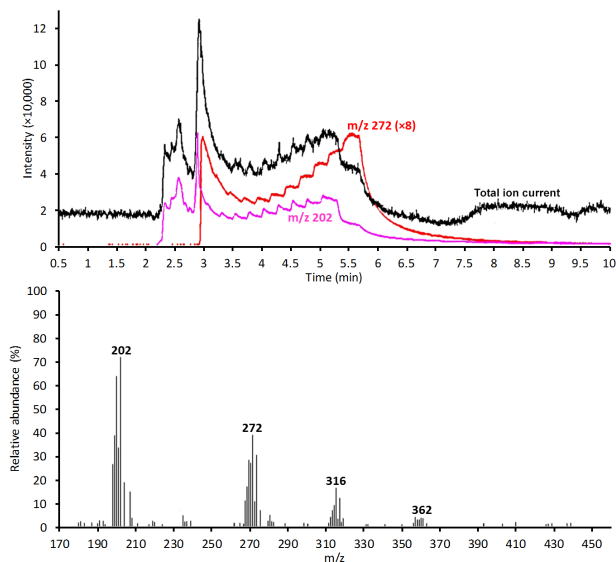


Figure 7. Chromatogram (above) and mass spectrum at 5.6 min (below) of HgCl_2 permeated onto quartz wool-filled PFA tubing, then desorbed into the GC/MS system.

The deactivated fused silica-coated stainless steel tube collected HgBr_2 with no discernable non-Hg interference, but the amount of HgBr_2 collected was low, probably because of high breakthrough. Deactivated fused silica-coated tubing may be a viable HgBr_2 collection device if a device with larger surface area is used and/or if the tubing is cooled to a temperature that limits Hg^{II} breakthrough.

3.6 Ambient air sample collection

The location, duration, and methods used for ambient air sample collection are given in Methods. None of the ambient air samples collected using quartz wool-filled tubes or nylon membranes resulted in any detectable Hg compounds. Low Hg^{II} concentrations in ambient air could have led to a sampled Hg^{II} mass below the detection limits of the GC/MS. 10.1 m^3 of ambient air was sampled by each nylon membrane, and 5.4 m^3 of air was sampled by each quartz wool-filled tube. These sampling volumes are adequate to collect $100 \text{ pg Hg}^{\text{II}}$ (within the detection limit of the GC/MS) if ambient Hg^{II} was 10 and 18 pg m^{-3} , respectively. Not all ambient air sample collections were associated with alternative Hg^{II} measurements, but for quartz wool-filled tube collection at the University of Nevada, Reno, Hg^{II} (measured by a Tekran 2537/1130/1135 speciation system as the sum of Hg collected on the system's denuder and particulate filter) was $38 \pm 9 \text{ pg m}^{-3}$ (mean $\pm 95\%$ confidence interval). However, some breakthrough may have occurred through the sample collection devices, and the non-Hg interference caused by the sample collection devices likely increased the actual detection limit for these samples. Alternatively, it is possible

that the Hg compounds in sampled ambient air were not Hg halides and were undetectable by the GC/MS system.

3.7 Future work

Improvements to the MS used in this work may increase its sensitivity for Hg compounds and decrease the detection limits of our system. Deeds et al. (2015) reported detection limits of 6–40 pg for HgCl₂ and HgBr₂ with an atmospheric pressure chemical ionization MS, and pointed out that chemical ionization is likely to decrease detection limits relative to electron impact ionization. The system used by Deeds et al. (2015), however, suffered from interference from non-Hg compounds found in ambient air because it did not utilize chromatographic separation. Our GC system, coupled with chemical ionization MS, may be able to achieve improved ambient air detection limits while maintaining the ability to separate individual Hg compounds and separate Hg compounds from non-Hg atmospheric constituents.

Interference in mass spectra created by collection materials likely limited our ability to detect Hg compounds in ambient air. Testing of additional collection materials is needed. Deeds et al. (2015) used shredded Teflon packed in tubes to collect Hg halides, and they did not note any interference from these materials. We found no interference from deactivated fused silica-coated stainless steel tubing. Highly inert surfaces like these are ideal because they do not result in off-gassing that may interfere with mass spectra. However, Hg^{II} may not collect efficiently on these surfaces unless they are cooled to 0 °C or lower. In addition, Lyman et al. (2010b) reported that ozone reduces Hg halides collected on uncoated quartz traps to Hg⁰, and highly inert surfaces may also leave Hg^{II} exposed to reaction with ozone or other atmospheric constituents.

We observed poor results from tubes packed with PDMS foam, but saw little interference from the PDMS-coated chromatographic column (for Hg halides). PDMS in chromatographic columns is cross-linked to stabilize it and is less likely to decompose. PDMS denuders have been used successfully to preconcentrate a wide variety of compounds (Burger et al., 1991; Dudek et al., 2002), including semivolatiles (Rowe and Perlinger, 2010). PDMS may also shield analytes from atmospheric oxidants that have low affinity for the PDMS phase (possibly including ozone) (Rowe and Perlinger, 2010).

While the GC/MS system in this study was able to separate and quantitatively analyze Hg halides, we have not yet shown that it can detect non-halide Hg compounds, including Hg(NO₃)₂ and HgO. HgO may not exist in the gas phase, but Hg(NO₃)₂ is likely to be non-polar, as are Hg halides (Goodsite et al., 2004), and likely can exist in the gas phase. HgBrX compounds, including HgBrOH, may exist in the atmosphere (Weiss-Penzias et al., 2015). HgBrOH, unlike HgBr₂, has an appreciable dipole moment (Goodsite et al., 2004) and may have different reactivity and volatility than HgBr₂. Our sys-

tem is able to detect HgBrCl, so it could possibly identify other bromine-containing Hg compounds, but this has not been tested. System temperatures and materials may need to be optimized for individual compounds or groups of compounds. Different Hg compounds may perform better with different columns, as shown by Babko et al. (2001). Finally, replacement of VICI valves (which have Valcon rotors that may react with Hg compounds) with all-stainless steel valves that can be coated with deactivated fused silica may improve system performance for Hg compounds that are more reactive than Hg halides.

4 Summary

Identification of atmospheric Hg^{II} is needed to improve understanding of Hg chemistry and biogeochemical cycling. The GC/MS-based system described here has a detection limit low enough to identify and quantify Hg halides in the ambient atmosphere, but better atmospheric sampling materials are needed to accomplish this. Work is ongoing to continue its development, including improving ambient air collection options, increasing the number of compounds it can reliably detect, and improving instrument sensitivity.

The Supplement related to this article is available online at doi:10.5194/amt-9-2195-2016-supplement.

Acknowledgements. Funding for this work was provided by US National Science Foundation award number 1324781 and the Electric Power Research Institute. We are grateful to Mae Gustin, Jiaoyan Huang, and Matthieu Miller at the University of Nevada, Reno, for collecting some of the ambient air samples used in this study and to Mae Gustin for providing helpful comments on the manuscript.

Edited by: P. Herckes

References

- Ariya, P. A., Peterson, K., Snider, G., and Amyot, M.: Mercury chemical transformations in the gas, aqueous and heterogeneous phases: state-of-the-art science and uncertainties, in: Mercury Fate and Transport in the Global Atmosphere, edited by: Mason, R. and Pirrone, N., Springer, New York, NY, USA, 2009.
- Babko, S. V., Monttgomery, J. L., Battleson, D. M., Whitworth, C. G., Sears, J., Summer, J., and Gingery, D.: Mercury Speciation Analysis by Gas Chromatography/Electron Impact/Mass Spectrometry, Waste Management Conference, 25 February–1 March 2001, Tucson, AZ, USA, 2001.
- Burger, B. V., Roux, M. L., Munro, Z. M., and Wilken, M. E.: Production and use of capillary traps for headspace gas chromatography of airborne volatile organic compounds, 18th International symposium on chromatography part I, 552, 137–151, 1991.

- Calvert, J. G. and Lindberg, S. E.: Mechanisms of mercury removal by O-3 and OH in the atmosphere, *Atmos. Environ.*, 39, 3355–3367, 2005.
- Carraher, C.: *Carraher's Polymer Chemistry*, 9th Edition, CRC Press, Boca Raton, FL, USA, 2014.
- Cavalheiro, J., Preud'homme, H., Amouroux, D., Tessier, E., and Monperrus, M.: Comparison between GC-MS and GC-ICPMS using isotope dilution for the simultaneous monitoring of inorganic and methyl mercury, butyl and phenyl tin compounds in biological tissues, *Anal. Bioanal. Chem.*, 406, 1253–1258, 2014.
- Deeds, D. A., Ghoshdastidar, A., Raofie, F., Gueïrette, E. A., Tessier, A., and Ariya, P. A.: Development of a Particle-Trap Preconcentration-Soft Ionization Mass Spectrometric Technique for the Quantification of Mercury Halides in Air, *Anal. Chem.*, 87, 5109–5116, 2015.
- de Laeter, J. R., Böhlke, J. K., De Bièvre, P., Hidaka, H., Peiser, H. S., Rosman, K. J. R., and Taylor, P. D. P.: Atomic weights of the elements: Review 2000 (IUPAC Technical Report), *Pure Appl. Chem.*, 75, 683–800, 2004.
- dos Santos, J. S., de la Guardia, M., Pastor, A., and dos Santos, M. L. P.: Determination of organic and inorganic mercury species in water and sediment samples by HPLC on-line coupled with ICP-MS, *Talanta*, 80, 207–211, 2009.
- Dudek, M., Kloskowski, A., Wolska, L., Pilarczyk, M., and Namiesnik, J.: Using different types of capillary chromatographic columns as denudation traps: a comparison of sorption properties, *J. Chromatogr. A*, 977, 115–123, 2002.
- Eagles-Smith, C. A. and Ackerman, J. T.: Mercury bioaccumulation in estuarine wetland fishes: Evaluating habitats and risk to coastal wildlife, *Environ. Pollut.*, 193, 147–155, 2014.
- Galbreath, K. C. and Zygarlicke, C. J.: Mercury transformations in coal combustion flue gas, *Fuel Process. Technol.*, 65, 289–310, 2000.
- Goodsite, M. E., Plane, J., and Skov, H.: A theoretical study of the oxidation of Hg⁰ to HgBr₂ in the troposphere, *Environ. Sci. Technol.*, 38, 1772–1776, 2004.
- Gratz, L., Ambrose, J., Jaffe, D., Shah, V., Jaeglé, L., Stutz, J., Festa, J., Spolaor, M., Tsai, C., and Selin, N.: Oxidation of mercury by bromine in the subtropical Pacific free troposphere, *Geophys. Res. Lett.*, 42, 10494–10502, 2015.
- Gustin, M. S., Lindberg, S. E., and Weisberg, P. J.: An update on the natural sources and sinks of atmospheric mercury, *Appl. Geochem.*, 23, 482–493, 2008.
- Gustin, M. S., Huang, J., Miller, M. B., Peterson, C., Jaffe, D. A., Ambrose, J., Finley, B. D., Lyman, S. N., Call, K., and Talbot, R.: Do we understand what the mercury speciation instruments are actually measuring? Results of RAMIX, *Environ. Sci. Technol.*, 47, 7295–7306, 2013a.
- Gustin, M. S., Huang, J. Y., Miller, M. B., Peterson, C., Jaffe, D. A., Ambrose, J., Finley, B. D., Lyman, S. N., Call, K., Talbot, R., Feddersen, D., Mao, H. T., and Lindberg, S. E.: Do We Understand What the Mercury Speciation Instruments Are Actually Measuring? Results of RAMIX, *Environ. Sci. Technol.*, 47, 7295–7306, 2013b.
- Hedgecock, I. M. and Pirrone, N.: Chasing quicksilver: Modeling the atmospheric lifetime of Hg⁰ (g) in the marine boundary layer at various latitudes, *Environ. Sci. Technol.*, 38, 69–76, 2004.
- Holmes, C. D.: Atmospheric chemistry: Quick cycling of quicksilver, *Nat. Geosci.*, 5, 95–96, 2012.
- Holmes, C. D., Jacob, D. J., and Yang, X.: Global lifetime of elemental mercury against oxidation by atomic bromine in the free troposphere, *Geophys. Res. Lett.*, 33, L20808, doi:10.1029/2006GL027176, 2006.
- Holmes, C. D., Jacob, D. J., Corbitt, E. S., Mao, J., Yang, X., Talbot, R., and Slemr, F.: Global atmospheric model for mercury including oxidation by bromine atoms, *Atmos. Chem. Phys.*, 10, 12037–12057, doi:10.5194/acp-10-12037-2010, 2010.
- Huang, J. and Gustin, M. S.: Uncertainties of Gaseous Oxidized Mercury Measurements Using KCl-Coated Denuders, Cation-Exchange Membranes, and Nylon Membranes: Humidity Influences, *Environ. Sci. Technol.*, 49, 6102–6108, 2015.
- Huang, J., Miller, M. B., Weiss-Penzias, P., and Gustin, M. S.: Comparison of gaseous oxidized Hg measured by KCl-coated denuders, and nylon and cation exchange membranes, *Environ. Sci. Technol.*, 47, 7307–7316, 2013a.
- Huang, J. Y., Miller, M. B., Weiss-Penzias, P., and Gustin, M. S.: Comparison of Gaseous Oxidized Hg Measured by KCl-Coated Denuders, and Nylon and Cation Exchange Membranes, *Environ. Sci. Technol.*, 47, 7307–7316, 2013b.
- Hynes, A. J., Donohoue, D. L., Goodsite, M. E., and Hedgecock, I. M.: Our current understanding of major chemical and physical processes affecting mercury dynamics in the atmosphere and at the air-water/terrestrial interfaces, in: *Mercury Fate and Transport in the Global Atmosphere*, edited by: Mason, R. and Pirrone, N., Springer, New York, NY, USA, 2009.
- Jaffe, D. A., Lyman, S., Amos, H. M., Gustin, M. S., Huang, J. Y., Selin, N. E., Levin, L., ter Schure, A., Mason, R. P., Talbot, R., Rutter, A., Finley, B., Jaegle, L., Shah, V., McClure, C., Ambrose, J., Gratz, L., Lindberg, S., Weiss-Penzias, P., Sheu, G. R., Feddersen, D., Horvat, M., Dastoor, A., Hynes, A. J., Mao, H. T., Sonke, J. E., Slemr, F., Fisher, J. A., Ebinghaus, R., Zhang, Y. X., and Edwards, G.: Progress on Understanding Atmospheric Mercury Hampered by Uncertain Measurements, *Environ. Sci. Technol.*, 48, 7204–7206, 2014.
- Johnson, D. L. and Braman, R. S.: Distribution of atmospheric mercury species near ground, *Environ. Sci. Technol.*, 8, 1003–1009, 1974.
- Laurier, F. J. G., Mason, R. P., Whalin, L., and Kato, S.: Reactive gaseous mercury formation in the North Pacific Ocean's marine boundary layer: A potential role of halogen chemistry, *J. Geophys. Res.-Atmos.*, 108, 4529, doi:10.1029/2003JD003625, 2003.
- Lin, C. J., Pongprueksa, P., Lindberg, S. E., Pehkonen, S. O., Byun, D., and Jang, C.: Scientific uncertainties in atmospheric mercury models I: Model science evaluation, *Atmos. Environ.*, 40, 2911–2928, 2006.
- Lindberg, S., Bullock, R., Ebinghaus, R., Engstrom, D., Feng, X. B., Fitzgerald, W., Pirrone, N., Prestbo, E., and Seigneur, C.: A synthesis of progress and uncertainties in attributing the sources of mercury in deposition, *Ambio*, 36, 19–32, 2007.
- L'Vov, B. V.: Kinetics and mechanism of thermal decomposition of mercuric oxide, *Thermochim. Acta*, 333, 21–26, 1999.
- Lyman, S. N. and Gustin, M. S.: Speciation of atmospheric mercury at two sites in northern Nevada, USA, *Atmos. Environ.*, 42, 927–939, 2008.
- Lyman, S. N. and Jaffe, D. A.: Formation and fate of oxidized mercury in the upper troposphere and lower stratosphere, *Nat. Geosci.*, 5, 114–117, 2012.

- Lyman, S. N., Gustin, M. S., Prestbo, E. M., and Marsik, F. J.: Estimation of Dry Deposition of Atmospheric Mercury in Nevada by Direct and Indirect Methods, *Environ. Sci. Technol.*, 41, 1970–1976, 2007.
- Lyman, S. N., Gustin, M. S., Prestbo, E. M., Kilner, P. I., Edger-ton, E., and Hartsell, B.: Testing and Application of Surrogate Surfaces for Understanding Potential Gaseous Oxidized Mercury Dry Deposition, *Environ. Sci. Technol.*, 43, 6235–6241, 2009.
- Lyman, S. N., Gustin, M. S., and Prestbo, E. M.: A passive sam-pler for ambient gaseous oxidized mercury concentrations, *Atmos. Environ.*, 44, 246–252, 2010a.
- Lyman, S. N., Jaffe, D. A., and Gustin, M. S.: Release of mer-cury halides from KCl denuders in the presence of ozone, *Atmos. Chem. Phys.*, 10, 8197–8204, doi:10.5194/acp-10-8197-2010, 2010b.
- Malcolm, E. G. and Keeler, G. J.: Evidence for a sampling artifact for particulate-phase mercury in the marine atmosphere, *Atmos. Environ.*, 41, 3352–3359, 2007.
- McClure, C. D., Jaffe, D. A., and Edgerton, E. S.: Evaluation of the KCl denuder method for gaseous oxidized mercury using HgBr₂ at an in-service AMNet site, *Environ. Sci. Technol.*, 48, 11437–11444, 2014.
- Obrist, D., Tas, E., Peleg, M., Matveev, V., Fain, X., Asaf, D., and Luria, M.: Bromine-induced oxidation of mercury in the mid-latitude atmosphere, *Nat. Geosci.*, 4, 22–26, 2011.
- Olson, E. S., Sharma, R. K., and Pavlish, J. H.: On the analysis of mercuric nitrate in flue gas by GC-MS, *Anal. Bioanal. Chem.*, 374, 1045–1049, 2002.
- Pacyna, E. G., Pacyna, J. M., Steenhuisen, F., and Wilson, S.: Global anthropogenic mercury emission inventory for 2000, *Atmos. Environ.*, 40, 4048–4063, 2006.
- Pal, B. and Ariya, P. A.: Gas-phase HO center dot-Initiated reactions of elemental mercury: Kinetics, product studies, and atmospheric implications, *Environ. Sci. Technol.*, 38, 5555–5566, 2004a.
- Pal, B. and Ariya, P. A.: Studies of ozone initiated reactions of gaseous mercury: kinetics, product studies, and atmospheric im-plications, *Phys. Chem. Chem. Phys.*, 6, 572–579, 2004b.
- Peleg, M., Tas, E., Matveev, V., Obrist, D., Moore, C. W., Gabay, M., and Luria, M.: Observational evidence for involvement of nitrate radicals in nighttime oxidation of mercury, *Environ. Sci. Technol.*, 49, 14008–14018, 2015.
- Peterson, S. H., Ackerman, J. T., and Costa, D. P.: Marine forag-ing ecology influences mercury bioaccumulation in deep-diving northern elephant seals, *P. Roy. Soc. B-Biol. Sci.*, 282, 26085591, doi:10.1098/rspb.2015.0710, 2015.
- Rowe, M. D. and Perlinger, J. A.: Performance of a High Flow Rate, Thermally Extractable Multicapillary Denuder for Atmospheric Semivolatile Organic Compound Concentration Measurement, *Environ. Sci. Technol.*, 44, 2098–2104, 2010.
- Schroeder, W. H., Anlauf, K. G., Barrie, L. A., Lu, J. Y., Steffen, A., Schneeberger, D. R., and Berg, T.: Arctic springtime depletion of mercury, *Nature*, 394, 331–332, 1998.
- Seigneur, C., Wrobel, J., and Constantinou, E.: A chemical kin-etic mechanism for atmospheric inorganic mercury, *Environ. Sci. Technol.*, 28, 1589–1597, 1994.
- Seigneur, C., Vijayaraghavan, K., Lohman, K., Karamchandani, P., and Scott, C.: Global source attribution for mercury deposition in the United States, *Environ. Sci. Technol.*, 38, 555–569, 2004.
- Selin, N. E.: Global Biogeochemical Cycling of Mercury: A Re-view, *Annu. Rev. Env. Resour.*, 34, 43–63, 2009.
- Shepler, B. C. and Peterson, K. A.: Mercury monoxide: A system-atic investigation of its ground electronic state, *J. Phys. Chem. A*, 107, 1783–1787, 2003.
- Slemr, F., Ebinghaus, R., Brenninkmeijer, C. A. M., Hermann, M., Kock, H. H., Martinsson, B. G., Schuck, T., Sprung, D., van Velthoven, P., Zahn, A., and Ziereis, H.: Gaseous mercury distri-bution in the upper troposphere and lower stratosphere observed onboard the CARIBIC passenger aircraft, *Atmos. Chem. Phys.*, 9, 1957–1969, doi:10.5194/acp-9-1957-2009, 2009.
- Sommar, J., Hallquist, M., Ljungstrom, E., and Lindqvist, O.: On the gas phase reactions between volatile biogenic mercury species and the nitrate radical, *J. Atmos. Chem.*, 27, 233–247, 1997.
- Sprovieri, F., Pirrone, N., Ebinghaus, R., Kock, H., and Dom-mergue, A.: Corrigendum to “A review of worldwide atmo-spheric mercury measurements” published in *Atmos. Chem. Phys.*, 10, 8245–8265, 2010, *Atmos. Chem. Phys.*, 10, 8531–8531, doi:10.5194/acp-10-8531-2010, 2010.
- Steffen, A., Douglas, T., Amyot, M., Ariya, P., Aspino, K., Berg, T., Bottenheim, J., Brooks, S., Cobbett, F., Dastoor, A., Dommergue, A., Ebinghaus, R., Ferrari, C., Gardfeldt, K., Goodsite, M. E., Lean, D., Poulain, A. J., Scherz, C., Skov, H., Sommar, J., and Temme, C.: A synthesis of atmospheric mercury depletion event chemistry in the atmosphere and snow, *Atmos. Chem. Phys.*, 8, 1445–1482, doi:10.5194/acp-8-1445-2008, 2008.
- Talbot, R., Mao, H., Scheuer, E., Dibb, J., and Avery, M.: Total de-pletion of Hg degree in the upper troposphere-lower stratosphere, *Geophys. Res. Lett.*, 34, L23804, doi:10.1029/2007GL031366, 2007.
- Tossell, J. A.: Calculation of the energetics for the oligomerization of gas phase HgO and HgS and for the solvolysis of crystalline HgO and HgS, *J. Phys. Chem. A*, 110, 2571–2578, 2006.
- Wang, F., Saiz-Lopez, A., Mahajan, A. S., Gómez Martín, J. C., Armstrong, D., Lemes, M., Hay, T., and Prados-Roman, C.: En-hanced production of oxidised mercury over the tropical Pacific Ocean: a key missing oxidation pathway, *Atmos. Chem. Phys.*, 14, 1323–1335, doi:10.5194/acp-14-1323-2014, 2014.
- Weiss-Penzias, P., Amos, H. M., Selin, N. E., Gustin, M. S., Jaffe, D. A., Obrist, D., Sheu, G.-R., and Giang, A.: Corrigendum to “Use of a global model to understand speciated atmospheric mer-cury observations at five high-elevation sites” published in *Atmos. Chem. Phys.*, 15, 1161–1173, 2015, *Atmos. Chem. Phys.*, 15, 2225–2225, doi:10.5194/acp-15-2225-2015, 2015.
- Widmer, N. C., West, J., and Cole, J. A.: Thermochemical study of mercury oxidation, 93rd Annual Meeting of the Air and Waste Management Association, 18–22 June 2000, Salt Lake City, Utah, USA, 2000.
- Wilcox, J. and Blowers, P.: Decomposition of Mercuric Chloride and Application to Combustion Flue Gases, *Environ. Chem.*, 1, 166–171, 2004.